1 Power Grid Network Analysis for Smart Grid Applications

Zhifang Wang, Anna Scaglione, and †Robert J. Thomas

University of California Davis, †Cornell University

Smart Grid is an umbrella term which refers to the modernization of electricity delivery systems with enhanced monitoring, analysis, control, and communication capabilities in order to improve the efficiency, reliability, economics, and sustainability of electricity services. The modernization happens at both the High Voltage (HV) transmission and the Medium or Low Voltage (MV/LV) distribution grids and aims at a diverse set of goals including facilitating greater competition between providers, encouraging greater use of alternative energy sources, implementing the automation and monitoring capabilities needed for bulk transmission, and enabling the use of market forces to drive energy conservation.

Many of the existing technologies already used by electric utilities will be taken full advantage of in Smart Grid but additional communication and control capabilities will also be established to optimize the operation of the entire electrical grid. Smart Grid is also positioned to adopt new technologies, such as smart metering, synchronous phasor measurement units (PMUs), plug-in hybrid electric vehicles (PHEVs), various forms of distributed generation, solar and wind energy, lighting management systems, distribution automation, and many more.

In order to design an efficient communication scheme and examine the efficiency of any networked control architecture in smart grid applications, we need to characterize statistically its information source, namely the power grid itself. Investigating the statistical properties of power-grids has the immediate benefit of providing a natural simulation platform, producing a large number of power grid test cases with realistic topologies, with scalable network size, and with realistic electrical parameter settings. The second benefit is that one can start analyzing the performance of decentralized control algorithms over information networks whose topology matches that of the underlying power network and use network scientific approaches to determine analytically if these architectures would scale well.

1.1 Introduction

This chapter provides a comprehensive study on the topological and electrical characteristics of a power grid transmission network based on a number of syn-

thetic and real-world power systems. Besides some basic graph theoretic metrics, it especially considers the following ones:

- *Small-World Properties*: The transmission network of a power grid is sparsely connected and manifests salient *small-world* properties which are characterized by the larger *clustering coefficient* and much smaller *average shortest path* compared with a random graph network with the same network size [1]. However, it is found that power grid assumes a different kind of *small-world* topology rather than that of the Watts-Strogatz *small-world* model.
- *Nodal Degree Distribution*: This metric reflects how the nodes in a power grid network connects with neighbors and closely relates with the network topology robustness under node removal [2][3]. Although most literature assumes that power grids have an exponential (or Geometric) nodal degree distribution [4][5], it is found that the empirical distribution estimated from real-world power systems clearly deviates from that of a exponential distribution, especially in the range of small node degrees. The probability generation function is applied to analyzing the node degree distribution and estimating the parameters for it.
- *Graph Spectrum and Connectivity Scaling Property*:The two metrics associate with the eigenvalues of the adjacency matrix and the Laplacian matrix respectively. And they carry important topology characteristics of a network.
- *Distribution of Line Impedance*: The line impedances dominates the electrical characteristics of a power grid network hence a study on its distribution is important and necessary. It is found that the distribution of line impedances is heavy-tailed and can be captured quite accurately by a clipped Double Pareto LogNormal (DPLN) distribution.

This chapter introduces an algorithm which is able to generate random topology power grids featuring the same topology and electrical characteristics found from the real data. Finally at the end of the chapter, it also reports recent studies on the topological and electrical characteristics of a sample medium-voltage (MV) power distribution network.

1.2   System Model

The power network dynamics are coupled by its network equation

$$YU = I, \tag{1.1}$$

where U and I represent the complex phasor vectors of bus voltages and injected currents; and Y is the network admittance matrix which is determined not only by the connecting topology but also its electrical parameters. Given a network with n nodes and m links (which may also be referred to as *buses* and *branches* or *lines* in power grid analysis; or *vertices* and *edges* in graph theory and network analysis), each link $l = (s, t)$ between nodes s and t has a line impedance $z_{pr}(l) =$

$r(l) + jx(l)$, where $r(l)$ is the resistance and $x(l)$ the reactance. Usually for high-voltage transmission network the reactance dominates, i.e., $x(l) \gg r(l)$. The line admittance is obtained from the inverse of its impedance, i.e., $y_{pr}(l) = g(l) + jb(l) = 1/z_{pr}(l)$.

Assume that a unit current flows along the link $l = (s,t)$ from node s to t; then the caused voltage difference between the ends of the link equals $\Delta u = U(s) - U(t) = z_{pr}(l)$ or equivalently $\Delta u = 1/y_{pr}(l)$. Therefore $z_{pr}(l)$ can be interpreted as the *electrical distance* between node s and t and $y_{pr}(l)$ reflects the *coupling strength* between the two end nodes.

Define the line-node incidence matrix $A := (A_{l,k})_{m \times n}$ as: $A_{l,s} = 1$, $A_{l,t} = -1$ if the lth link is between nodes s and t with arbitrary directions; and $A_{l,k} = 0$ otherwise. Then the network admittance matrix $Y := (Y_{s,t})_{n \times n}$ can be obtained as

$$Y = A^T diag(\mathbf{y_{pr}}) A, \tag{1.2}$$

with entries like below:

$$\begin{cases} Y(s,t) = -y_{pr}(s,t), & \text{if link } s - t \text{ exists, for } t \neq s \\ Y(s,s) = \sum_{t \neq s} y_{pr}(s,t), \\ Y(s,t) = 0, & \text{otherewise.} \end{cases} \tag{1.3}$$

The network Laplacian $L := (L_{s,t})_{n \times n}$ can then be obtained as $L = A^T A$, with entries as:

$$\begin{cases} L(s,t) = -1, \text{ if link } s - t \text{ exists, for } t \neq s \\ L(s,s) = k, \text{ with } k = deg(s) = \sum_{t \neq s} -L(s,t) \\ L(s,t) = 0, \text{ otherewise.} \end{cases} \tag{1.4}$$

A close comparison of the matrix structures of L and Y uncovers some interesting analogies. The Laplacian matrix L fully describes the topology of a network; while the network admittance matrix Y not only contains information about the system topology but also information about its electrical coupling. The off-diagonal entries of Y, $Y_{s,t}$ equals the line admittance of the link between node s and t (with a '$-$' sign), whose magnitude reflects the coupling strength between the two nodes. The diagonal entries of the Laplacian L represent the total number of links connecting each node with the rest of the network. Whereas a diagonal entry of Y represents the total coupling capability one node has with the rest of the network. Therefore the network admittance matrix Y can be viewed as a complex-weighted Laplacian; and the Laplacian L can be equivalent to a "flat" network admittance matrix, which assumes all the links in the network have the same line impedance (with a common proportional factor).

1.3   Topology Measures of Power Grids

First we look at some basic topological metrics for a power grid network, i.e. the network size n, the total number of links m, the average nodal degree $\langle k \rangle$, the average shortest path length counted in hops $\langle l \rangle$, and the Pearson coefficient. All these metrics can be derived from the Laplacian matrix:

- *The total number of links*: is $m = \frac{1}{2} \sum_i L(i,i)$;
- *The average nodal degree*: is $\langle k \rangle = \frac{1}{n} \sum_i L(i,i)$;
- *The network adjacency matrix*: can be obtained as $M_{adj} = -L + diag\{L\}$;
- *The the average shortest path $\langle l \rangle$ measured in hops*: can be calculated with the the Dijkastra's algorithm [6] based on M_{adj}.

Define the nodal degree vector as $\underline{k} = [k_1, k_2, \cdots, k_n] = \text{diag}(L)$. And $\overline{k}$ is the average degree of a node seen at the end of a randomly selected link (i,j), i.e.,

$$\overline{k} = (2m)^{-1} \sum_{(i,j)} (k_i + k_j) = (2m)^{-1} \sum_i k_i{}^2 = \frac{\langle k^2 \rangle}{\langle k \rangle}. \tag{1.5}$$

Thus we can compute the Pearson coefficient of node degrees of the network as

$$\rho = \frac{\sum_{(i,j)} (k_i - \overline{k})(k_j - \overline{k})}{\sqrt{\sum_{(i,j)} (k_i - \overline{k})^2 (k_j - \overline{k})^2}}, \tag{1.6}$$

which is a measure of the correlation of node degrees in the network[7].It has been observed that the Pearson coefficient for some kinds of networks is consistently positive while for other kinds it is negative [8]. Therefore, some researchers proposed to use the Pearson coefficient to differentiate technological networks from social networks [9]. However, it is found that the Pearson coefficient of power grids does not have restrictive characteristics but ranges over a wide interval from negative and positive, which can be verified by the metric evaluation results listed in Table 1.1.

Power grids have been found to have the salient features of *small world graphs* (see the work by Watts and Strogatz [1]). That is, while the vast majority of links are similar to that of a regular lattice, with limited near neighbor connectivity, a few links connect across the network. These bridging links significantly shorten the path length that connects every two nodes and critically increase the connectivity of the network. At the same time, their scarcity puts the connectivity at risk in the case of link failure for one of these critical bridges. The characterizing measure to distinguish a *small-world* network is called *clustering coefficient*, which assesses the degree to which nodes tend to cluster together. A *small world* network usually has a clustering coefficient significantly higher than that of a random graph network, given the comparable network size and total number of edges. The random graph network mentioned here refers to the network model defined by Erdös-Rényi, with n labeled nodes connected by m

Table 1.1. Topological Metrics of the IEEE and Real-World Power Grid Networks

	(n, m)	$\langle l \rangle$	$\langle k \rangle$	ρ	$C(G)$	$C(R)$
IEEE-30	(30,41)	3.31	2.73	-0.0868	0.2348	0.094253
IEEE-57	(57,78)	4.95	2.74	0.2432	0.1222	0.048872
IEEE-118	(118,179)	6.31	3.03	-0.1526	0.1651	0.025931
IEEE-300	(300, 409)	9.94	2.73	-0.2206	0.0856	0.009119
NYISO	(2935,6567)	16.43	4.47	0.4593	0.2134	0.001525
WSCC	(4941, 6594)	18.70	2.67	0.0035	0.0801	0.000540

edges which are chosen uniformly randomly from the $n(n-1)/2$ possible edges [12].

The clustering coefficient is defined as the average of the clustering coefficient for each node [1]:

$$C(G) = \frac{1}{n} \sum_{i=1}^{n} C_i \tag{1.7}$$

with C_i being the node clustering coefficient as $C_i = \lambda_G(i)/\tau_G(i)$, where $\lambda_G(i)$ is the number of edges between the neighbors of node i and $\tau_G(i)$ the total number of edges that could possibly exist among the neighbors of node i. For undirected graphs, obviously $\tau_G(i) = k_i(k_i - 1)/2$ given k_i is the node degree. As pointed out in [10], the clustering coefficient for a random graph network theoretically equals the probability of randomly selecting links from all possible links. That is,

$$C(R) = \frac{m}{n(n-1)/2} = \frac{\langle k \rangle}{n-1}. \tag{1.8}$$

1.3.1 Topological Metrics

The topology metrics evaluated for the IEEE model systems, the NYISO and the WSCC systems have been shown in Table 1.1. Especially we show the clustering coefficients of the IEEE power systems, the NYISO, and the WSCC system compared to the random graph networks with same network size and same total number of links. The former is denoted as $C(G)$, and the latter as $C(R)$. For the reader's reference, the IEEE 30, 57, and 118 bus systems represent different parts of the American Electric Power System in the Midwestern US; the IEEE 300 bus system is synthesized from the New England power system. More information can be obtained from [16]. The Western System Coordinating Council (WSCC) grid is the interconnected system of transmission lines spanning the western United States plus parts of Canada and Mexico, and the NYISO system represents New York state bulk electricity grid.

From the table shown above one can observe two interesting properties pertaining to the topology of the grid: (a) the connectivity is very sparse, since the average nodal degree does not scale up, as the network size increases. Instead the average nodal degree falls into a very restricted range, which is more related with the particular geographical area where the network belongs to, rather than the network size. For example, power grids in western US have an average nodal degree between 2.5 and 3, while in northeastern US the power grids are a little denser with $\langle k \rangle$ around 4.5. (b) it is not accurate to attribute "small-world" features to power grids of any size. It is true that the samples we studied have a clustering coefficient significantly larger than that of a comparable-size random graph network. However, as we will discuss next, while being similarly sparse, power grids have better connectivity scaling laws than the *small-world* graphs proposed in [1].

1.3.2   The Small-World Wiring

The Watts-Strogatz *Small-world* model is generated starting from a regular ring lattice, then by using a small probability, rewiring some local links to an arbitrary node chosen uniformly at random in the entire network (to make it a *small-world* topology). A tool to visually highlight *small-world* topologies is the Kirk graph, which was proposed by J. Kirk (2007) [14]. It is a simple but effective way to show a network topology: First, node numbers are assigned according to physical nodal adjacency, that is, physically closely located nodes are given close numbers; then all the nodes are sequentially and evenly spread around a circle and links between nodes are drawn as straight lines inside the circle. Fig. 1.1 below shows three representative network topologies, using Kirk graphs, of an Erdös-Rényi Rand-graph network, of a Watts-Strogatz Small-world network, and of a realistic power grid – IEEE-57 network. The three networks have same network size and almost same total number of links. The topology difference between the Erdös-Rényi network and IEEE-57 network can be easily noticed in contrast to a good degree of similarity between the Watts-Strogatz *small-world* model and the test power network.

However, the rewiring of the test power grid is not independent, as in that of the Watts-Strogatz *small-world* model; instead, long hauls appear over clusters of nodes. This property is is visually noticeable in the IEEE 57 network and differentiates it from the *small-world* graph, where these links are chosen independently. This fact has an intuitive explanation: long hauls require having a right of way to deploy a long connection and it is highly likely that the long wires will reuse part of this space. These physical and economical constraints inevitably affect the structure of the topology. Besides, there is more than what meets the eyes. Watts-Strogatz *Small-world* model has scaling property that cannot be validated by power grid topologies, precisely because the average nodal degree of a power network is almost invariant to the size of the network. Given a network size with its specified average nodal degree, the model fails to produce
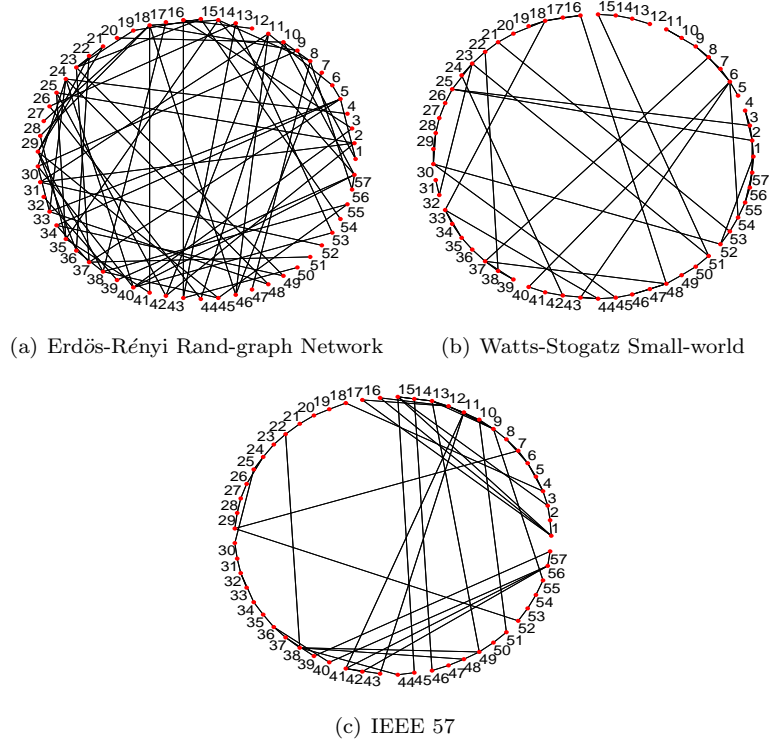
(a) Erdös-Rényi Rand-graph Network   (b) Watts-Stogatz Small-world

(c) IEEE 57

Figure 1.1 Topology Comparison Using Kirk Plot

a connected grid topology for reasonably large network sizes with realistic power grid degree distributions. The main reason for the poor scaling lies in the fact that in order to produce a sparse but connected topology, the Watts-Strogatz *Small-world* model requires [1][10]:

$$1 \ll \ln(n) \ll \langle k \rangle \ll n \tag{1.9}$$

or equivalently as $\langle k \rangle \ll n \ll e^{\langle k \rangle}$. On the other hand, real-world power grids have a very low average nodal degree with $\langle k \rangle = 2 \sim 5$, regardless of the network size. This will limit the network size much smaller than 150 in order to produce a connected topology using the model. However, in the real world, large power grids are connected even if they are much sparser than what is required by the Watts-Strogatz *Small-world* model.

1.3.3   The Nodal Degree Distribution

Now we examine the empirical distribution of nodal degrees in the available real-world power grids. Fig. 1.3(a) shows the histogram probability mass function (PMF) in log-scale for the nodal degrees of NYISO system. If the PMF curve approximates a straight line in the semi-logarithm plot (i.e., shown as $\log(p(k))$

vs. k), it implies an exponential tail which is analogous to that of the Geometric distribution. However, it is also noticed that for the range of small node degrees, that is, when $k \leq 3$, the empirical PMF curve clearly deviates from that of a Geometric distribution.

The probability generation function (PGF) can be utilized to analyze the node degree distribution in power grids. The PGF of a random variable X is defined as $G_X(z) = \sum_k \Pr_{(x=k)} z^k$. Given a sample data set of X with the size of N, its PGF can also be estimated from the mean of z^X because

$$
\begin{aligned}
E(z^X) &= \frac{1}{n} \sum_x z^x \\
&= \frac{1}{n} \sum_k n_{(x=k)} z^k \\
&= \sum_k \frac{n_{(x=k)}}{n} z^k \\
&\approx \sum_k \Pr_{(x=k)} z^k
\end{aligned}
\tag{1.10}
$$

where $n_{(x=k)}$ denotes the total number of the data items equaling to k. Due to $\lim_{n \to \infty} \frac{n_{(x=k)}}{n} = \Pr_{(x=k)}$, we can have $E(z^X) \approx G_X(z)$ with a large enough data size.

If a random variable can be expressed as a sum of two independent random variables, its probability mass function (PMF) is then the convolution of the PMFs of the components variables, and its probability generation function (PGF) is the product of that of the component variables. That is,

$$
\begin{aligned}
X &= X_1 + X_2 \\
\Pr_{(X=k)} &= \Pr_{(X_1=k)} \otimes \Pr_{(X_2=k)} \\
G_X(z) &= G_{X_1}(z) G_{X_2}(z)
\end{aligned}
\tag{1.11}
$$

It is found that the node degree distribution in power grids can be very well approximated by a sum of two independent random variables, that is,

$$
\mathcal{K} = \mathcal{G} + \mathcal{D},
\tag{1.12}
$$

where $\mathcal{G}$ is a truncated Geometric with the threshold of k_{max}

$$
\begin{aligned}
\Pr_{(\mathcal{G}=k)} &= \frac{(1-p)^k p}{\sum_{i=0}^{k_{max}} (1-p)^i p} \\
&= \frac{(1-p)^k p}{1-(1-p)^{k_{max}+1}}, \quad k = 0, 1, 2, \cdots, k_{max}
\end{aligned}
\tag{1.13}
$$

with the PGF as

$$
\begin{aligned}
G_{\mathcal{G}}(z) &= \frac{\sum_{k=0}^{k_{max}} (1-p)^k p z^k}{1-(1-p)^{k_{max}+1}} \\
&= \frac{p\big(1-((1-p)z)^{k_{max}+1}\big)}{(1-(1-p)^{k_{max}+1})(1-(1-p)z)}
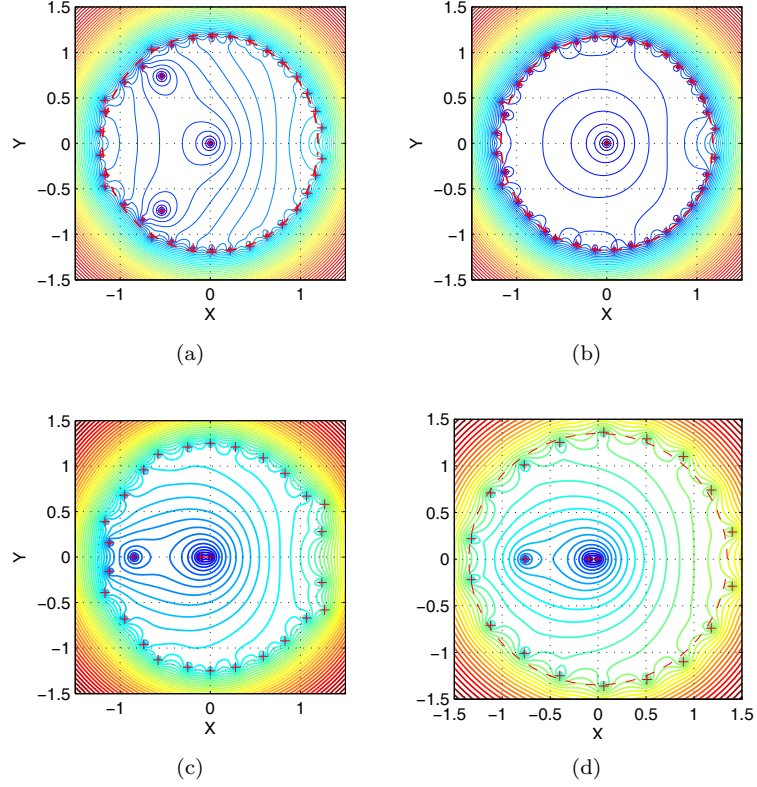\end{aligned}
\tag{1.14}
$$

Figure 1.2 The Contour Plot of $E(z^X)$ of Node Degrees for Different Groups of Buses in the NYISO system: (a) All buses; (b) Gen buses; (c) Load buses; (d) Connection buses; the zeros are marked by red '+'s.

And $\mathcal{D}$ is an irregular Discrete $\{p_1, p_2, \cdots, p_{k_t}\}$, with $\mathrm{Pr}_{(\mathcal{D}=k)} = p_k$, $\quad k = 1, 2, \cdots, k_t$ whose PGF is $G_{\mathcal{D}}(z) = p_1 z + p_2 z^2 + p_3 z^3 + \cdots + p_{k_t} z^{k_t}$. Therefore the PMF of $\mathcal{K}$ is $\mathrm{Pr}_{(\mathcal{K}=k)} = \mathrm{Pr}_{(\mathcal{G}=k)} \otimes \mathrm{Pr}_{(\mathcal{D}=k)}$. And the PGF of $\mathcal{K}$ can be written as

$$G_{\mathcal{K}}(z) = \frac{p \left(1 - ((1-p)z)^{k_{max}+1}\right) \sum_{i=1}^{k_t} p_i z^i}{\left(1 - (1-p)^{k_{max}+1}\right)\left(1 - (1-p)z\right)} \tag{1.15}$$
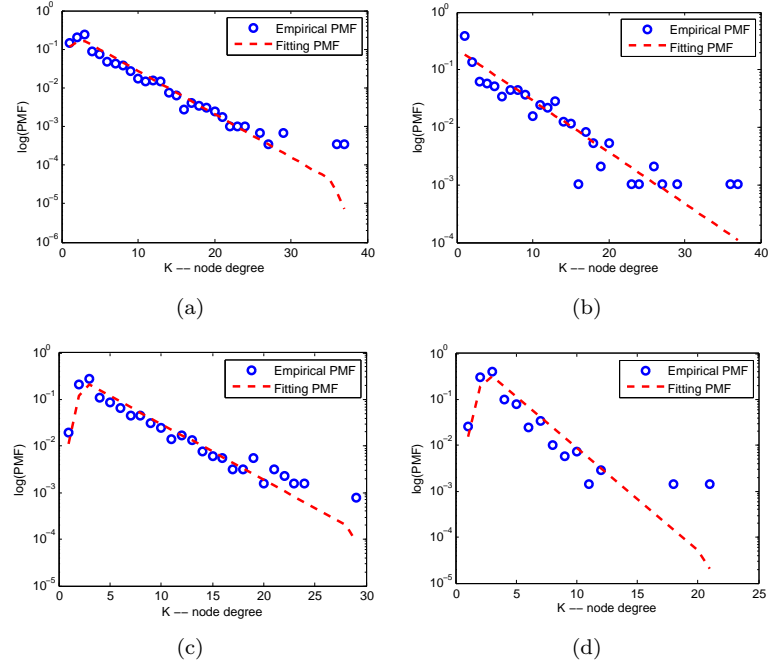
The equation (1.15) indicates that the PGF $G_{\mathcal{K}}(z)$ has k_{max} zeros evenly distributed around a circle of radius of $1/(1-p)$ which are introduced by the truncation of the Geometric $\mathcal{G}$ (because the zero at $1/(1-p)$ has been neutralized by the denominator $(1 - (1-p)z)$ and has k_t zeros introduced by the irregular Discrete $\mathcal{D}$ with $\{p_1, p_2, \cdots, p_{k_t}\}$.

Fig. 1.2 show the contour plots of PGF of node degrees for different groups of buses in the NYISO system. Three interesting discoveries are worth to note: (a) Clearly each plot contains evenly distributed zeros around a circle, which indicate a truncated Geometric component; (b) Besides the zeros around the

Table 1.2. Estimate Coefficients of the Node Degree Probability Density Functions of the NYISO and WSCC systems

node groups	k_{max}	$\max(\underline{k})$	k_t	p	$\{p_1, p_2, \cdots, p_{k_t}\}$
All	34	37	3	0.2269	0.4875, 0.2700, 0.2425
Gen	36	37	1	0.1863	1.000
Load	26	29	3	0.2423	0.0455, 0.4675, 0.4870
Conn	18	21	3	0.4006	0.0393, 0.4442, 0.5165
All-WSCC	16	19	3	0.4084	0.3545, 0.4499, 0.1956

circle, most contour plots also have a small number of off-circle zeros, which come from an embedding irregular Discrete component; (c) The contour plot for each group of nodes has zeros with similar pattern but different positions. This implies that each group of node degrees has similar distribution functions but with different coefficients. Therefore it is necessary and reasonable to characterize the node degrees distribution according to the node types. Otherwise if the node degrees aggregate into one single group, just as in Fig. 1.2(a), some important characteristics of a subgroup of node degrees would be concealed (e.g., comparing (a) and (b)-(d) in Fig. 1.2).

Figure 1.3 Comparing the Empirical and Fitting PMF of Node Degrees in the NYISO system: (a) all buses; (b) Gen buses; (c) Load buses; (d) Connection buses

Based on the contour plots one can easily locate the zeros in PGF, and further determine the coefficients of corresponding distribution functions. The estimated coefficients for each group of nodes in the NYISO and all the nodes in the WSCC systems are listed in the Table 1.2. Because the WSCC system data we have only contains un-weighted raw data without distinguishing node types, its node degree distribution is only analyzed for one aggregate group. Fig. 1.3 compares the probability mass function (PMF) with estimate coefficients and the empirical PMF of the NYISO system and shows that the former matches the latter with quite good approximation. The results from both systems have validated our assumption of node degree distribution in power grids: it can be expressed as a sum of a truncated Geometric random variable and an irregular Discrete random variable. And the results also demonstrated the effectiveness of the proposed method of analyzing node degree distribution by using the probability generation function.

1.3.4   The Graph Spectrum and The Scaling of Connectivity

The eigenvalues of the adjacency matrix M_{adj} and the Laplacian matrix L carry important topological features of a network. The two matrices are in fact exchangeable, and either of them fully describes a network topology. The set of eigenvalues of its adjacency matrix M_{adj} is called the spectrum of a graph . *Graph spectral density* is defined as:

$$\rho(\lambda) = \frac{1}{n} \sum_{j=1}^{n} \delta(\lambda - \lambda_j) \tag{1.16}$$

with $\{\lambda_j, j = 1, 2, \cdots, n\}$ forming the graph spectrum of the network. The kth moments of $\rho(\lambda)$ represents the average number of k-hop paths returning to the same node in the graph [10]. However, please note that these paths can contain nodes which are already visited. The *Graph spectral density* of network topology from different categories has distinctively different patterns [10]. A Erdös-Rényi random graph network $G(n; p)$, given a large network size n and a non-trivial link selection probability $p(n) = cn^{-z}$, with $z < 1$ and c as a constant regardless of network size, has its normalized spectral density converging to a semicircular distribution as $n \to \infty$. This is known as Wigner's semicircle law [20] [21]. That is:

$$\rho(\lambda) = \begin{cases} \frac{\sqrt{4-(\lambda/\lambda_0)^2}}{2\pi\lambda_0} & \text{if } |\lambda| < 2\lambda_0 \\ 0 & \text{otherwise} \end{cases} \tag{1.17}$$

with $\lambda_0 = \sqrt{np(1-p)}$ and $p = \frac{m}{n(n-1)/2} = \frac{\langle k \rangle}{n-1}$, where m is the total number of links and $\langle k \rangle$ is the average node degree. And $\widetilde{\rho} = 2\pi\lambda_0\rho(\lambda) = \sqrt{4 - \widetilde{\lambda}^2}$ with $\widetilde{\lambda} = \lambda/\lambda_0$ depicts a semi-circle around the origin with a radius of 2.

Next we refer to *spectrum* as the set of eigenvalues and to *spectral density* as its density of values. Fig. 1.4 shows the spectral density of a ring lattice (a),
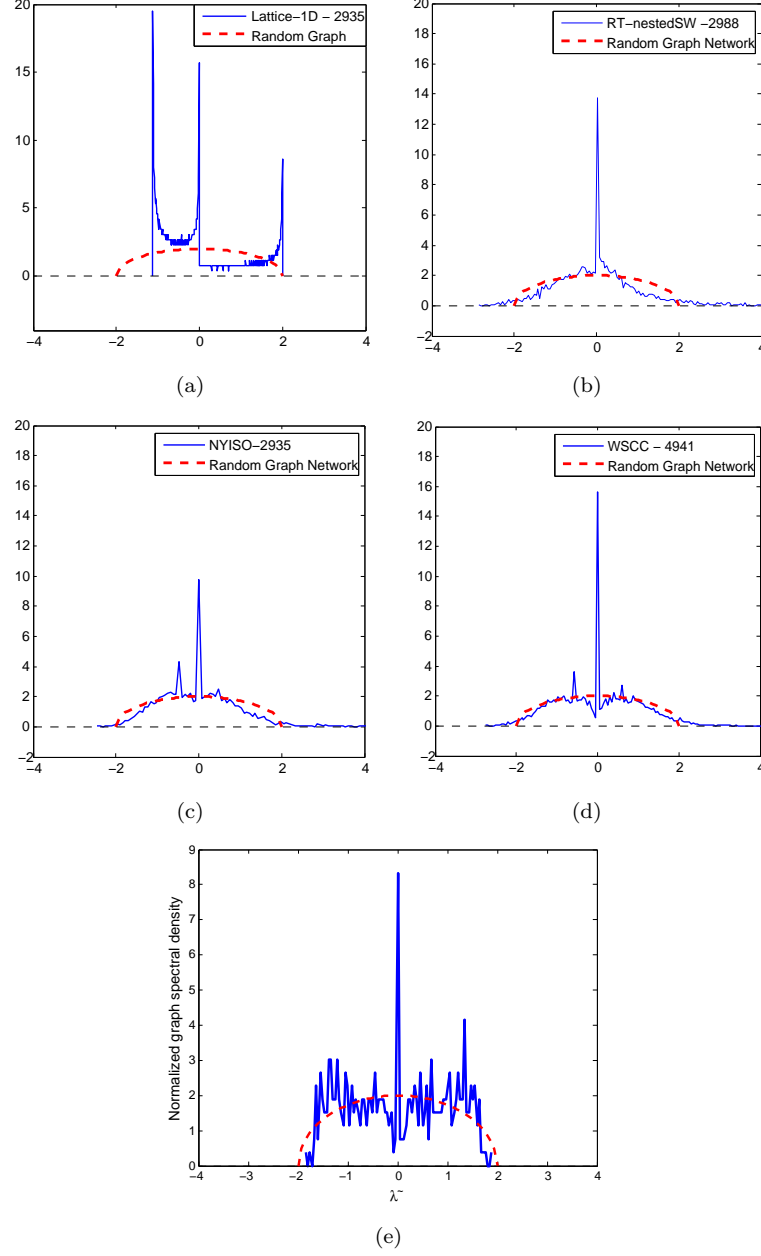
Figure 1.4 The Normalized Graph Spectral Density of Different Networks, $\widetilde{\rho}(\lambda)$ vs. $\widetilde{\lambda}$: the dotted line of semi-circle represents the graph spectral density of random graph networks; (a) A Ring Lattice; (b) RT-*nested-Smallworld*; (c) NYISO; (d) WSCC; (e) a 396-node MV distribution network .

of two real-world power grids (b) and (c), and of a power grid generated from the proposed RT-*nested-Smallworld* model (d), compared to the semi-circle law

Table 1.3. Algebraic Connectivity of the IEEE and Real-World Power Networks

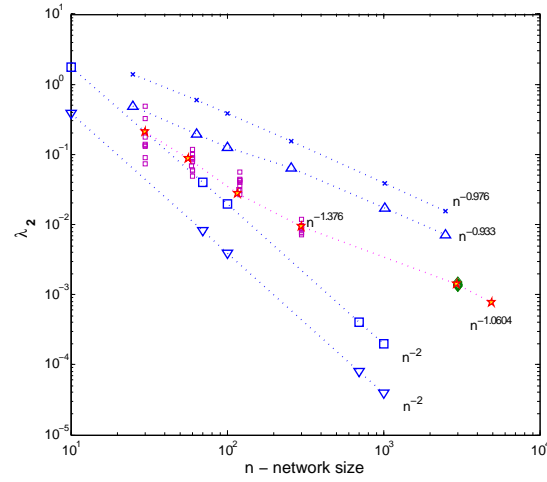|	n	$\lambda_2(L)$
IEEE-30	30	0.21213
IEEE-57	57	0.088223
IEEE-118	118	0.027132
IEEE-300	300	0.0093838
NYISO	2935	0.0014215
WSCC	4941	0.00075921

Figure 1.5 Connectivity Scaling Curve versus Network Size: 2D lattice with $k = 4$ (blue x-dotted line); 2D lattice with $k = 2$ (blue $\triangle$-dotted line); 1D lattice with $k = 4$ (blue $\square$-dotted line); 1D lattice with $k = 2$ (blue ∇-dotted line); nested-Smallworld RT with subnetwork-size= 30 (small darkred $\square$); nested-Smallworld RT with subnetwork-size= 300 (green $\diamondsuit$); Power Grids (red star).

corresponding to random graphs with the same network size and number of links. The plots demonstrate that power grid graphs have a very distinctive spectral density, far from that of regular or completely random networks; it also shows that the proposed model RT-*nested-Smallworld* (see section 1.5) is in good agreement with the real data in terms of graph spectral density.

Another important measure is the second smallest eigenvalue of the Laplacian matrix, $\lambda_2(L)$, called the algebraic connectivity. This measure is sometimes termed as Fiedler eigenvalue, due to the fact that it was first introduced by Fiedler (1989) [13]. $\lambda_2(L)$ reflects how well a network is connected and how fast information data can be shared across the network. As a fact the smallest eigenvalue of the Laplacian is always zero, i.e., $\lambda_1(L) \equiv 0$ and the number of times

0 appears as an eigenvalue in the Laplacian is the total number of connected components in the network. The eigenvalue $\lambda_2(L)$ is greater than 0 if and only if network is a connected graph. If the algebraic connectivity $\lambda_2(L)$ is close to zero, the network is close to being disconnected. Otherwise, if $\frac{1}{n}\lambda_2(L)$ tends to be 1, with n as the network size, the network tends to be fully connected.

Table 1.3 shows the algebraic connectivity of IEEE model systems and the NYISO system. Fig. 1.5 plots the connectivity scaling curve of power grid versus network size and compares it with that of 1-Dimensional and 2-Dimensional lattices. 1D-lattice is a ring structured topology, with nodes connected with most adjacent neighbors on both sides. 2D-lattice is a regular two-dimension meshed grid with each boundary side merging with the other side and each node connected to the most adjacent neighbors around it. For 1-D lattice, its connectivity scales as $\lambda_2(L) \propto n^{-2}$; for 2-D lattice , its connectivity grows as $\lambda_2(L) \propto n^{-1}$; interestingly, for power grids, its connectivity grows as $\lambda_2(L) \propto n^{-1.376 \sim -1.0604}$, lying between those of 1-D lattice and 2-D lattice.

In trying to fit the random wiring of power network we postulate a new possible model, RT-*nested-Smallworld*, in section 1.5. The model is resulted from nesting several "*small world*" sub-networks, whose size is likely to produce a connected topology with a realistic degree distribution, into a regular lattice again.More details can be found in section 1.5. The intuition guiding this modeling is that the network would have produced connected topologies with a connectivity that was intermediate between the 1- and 2-dimensional lattices. And Fig. 1.5 shows an excellent match between the algebraic connectivity of this type of model and the real data.

1.4   Line Impedance Distribution

This chapter not only examines the network topology of a power grid but makes efforts to reproduce accurately its electrical characteristics as well. Because the key element for a power grid network is its network admittance matrix Y, which associates both with the connecting topology and with its line impedances. The transmission line impedance in a power grid is in fact a complex number.

When it comes to the statistical analysis, we study the distribution of the magnitude of Z_{pr}. The line impedance can be represented as $Z_{pr} = R + jX$, where R is the resistance and X the reactance. Usually X is the dominant component, whereas R only takes a trivial value which in many cases can even be neglected. Therefore, one can easily reconstruct the complex value of Z_{pr} given its magnitude. The empirical data on line impedances of power grids are taken from IEEE model systems and the NYISO system. The first clear observation from the empirical histogram probability density distribution (PDF) is that the distribution of the line impedances is heavy-tailed. The candidate distribution functions include Gamma, Generalized Pareto (GP), Lognormal, Double-Pareto-Lognormal (DPLN), and two new distributions that we call Lognormal-clip, and

DPLN-clip, which will be explained later. In searching among the heavy tailed distributions for a fit, the parameters of the candidate distribution can be estimated via the maximum likelihood (ML) criterion from the data and the appropriately modified Kolmogorov-Smirnov test (K-S test) be used to check if the hypothesized distribution is a good fit.

The DPLN distribution was introduced by Reed and Jorgensen (2004) [17], which proved to be very useful to model the size distributions of various phenomena, like incomes and earnings, human settlement sizes, etc. We choose the the DPLN distribution as a candidate to fit the line impedance data in a power grid because the latter implicitly relate to human settlement size in the network. Generally speaking, large generation is usually located near water or the fuel source, but remotely away from densely populated area with large scale human settlements. Therefore long-distance transmission lines have been constructed in order to provide the interconnection and serve the large scale settlements. And the long-distance lines usually exhibit large line impedance.

The Lognormal-clip and DPLN-clip are especially suited for fitting the NYISO data because the line impedances in this system appear to approximate a Lognormal or DPLN distribution very well except for having an *interrupted* tail, which is captured by the *clipping*. Therefore it can be assumed that the NYISO data is resulted from some original impedance data being "*clipped*" by an exponential cutoff tailing coefficient. That is, given the original impedance data Y following a specific distribution, $Y \sim f_Y(y)$, the clipped impedance data is $X = Z_{\max}\left(1 - e^{-\frac{Y}{Z_{\max}}}\right)$, with $Z_{\max}$ being the cutoff threshold, so that $Y = -Z_{\max}\log\left(1 - \frac{X}{Z_{\max}}\right)$. And the resulting clip-distribution turns out to be

$$X \sim f_X(x) = Y'_{(x)}f_Y\left(Y_{(x)}\right)$$
$$= \frac{Z_{\max}}{Z_{\max} - x}f_Y\left(-Z_{\max}\log(1 - x/Z_{\max})\right) \qquad (1.18)$$

It is reasonable to introduce the clipping mechanism into the line impedance distribution because in real-world power grids, transmission lines are limited in length and, correspondingly, in the line impedance, which is proportional to the length. As shown next, the line impedances in real-world power grids have heavy-tailed distributions. Hence, the candidate distribution functions listed below, are selected in the class of heavy-tailed distributions:

Gamma:

$$\Gamma(x|a,b) = \frac{1}{b^a\Gamma(a)}x^{a-1}e^{x/b} \qquad (1.19)$$

Generalized Pareto (GP):

$$gp(x|k,\sigma,\theta) = \left(\frac{1}{\sigma}\right)\left(1 + k\frac{(x-\theta)}{\sigma}\right)^{-1-\frac{1}{k}} \qquad (1.20)$$

Lognormal:

$$logn(x|\mu,\sigma) = \frac{1}{x\sigma\sqrt{2\pi}}e^{\frac{-(\log x - u)^2}{2\sigma^2}} \tag{1.21}$$

Double-Pareto-Lognormal (DPLN):

$$
\begin{aligned}
dPlN&(x|\alpha,\beta,\mu,\sigma) \\
&= \tfrac{\alpha\beta}{\alpha+\beta}\Big[A(\alpha,\mu,\sigma)x^{-\alpha-1}\Phi\big(\tfrac{\log x - \mu - \alpha\sigma^2}{\sigma}\big) \\
&\quad + A(-\beta,\mu,\sigma)x^{\beta-1}\Phi^c\big(\tfrac{\log x - \mu + \beta\sigma^2}{\sigma}\big)\Big]
\end{aligned}
\tag{1.22}
$$

where $A(\theta,\mu,\sigma) = e^{(\theta\mu+\theta^2\sigma^2/2)}$.

Lognormal-clip:

$$
\begin{aligned}
logn&_{clip}(x|\mu,\sigma,Z_{\max}) \\
&= \tfrac{Z_{\max}}{Z_{\max}-x}logn\Big(-Z_{\max}\log(1-\tfrac{X}{Z_{\max}})|\mu,\sigma\Big)
\end{aligned}
\tag{1.23}
$$

DPLN-clip:

$$
\begin{aligned}
dPlN&_{clip}(x|\alpha,\beta,\mu,\sigma,Z_{\max}) \\
&= \tfrac{Z_{\max}}{Z_{\max}-x}dPlN\Big(-Z_{\max}\log(1-\tfrac{X}{Z_{\max}})|\alpha,\beta,\mu,\sigma\Big)
\end{aligned}
$$

$$\tag{1.24}$$

For each candidate distribution function one can estimate its parameters using the Maximum Likelihood (ML) method, and then run the Kolmogorov-Smiroff (K-S) test in order to pick the distribution which gives the best K-S test result. Table 1.4 shows the best-fitting distribution functions with the corresponding ML parameter estimates. Fig. 1.6 compares the empirical PDFs and CDFs (in logarithm scales) with those from best-fitting distribution function for the NYSIO system. The studies show that Gamma distribution is the best fit for the line impedances in the IEEE 30 and 118 systems and GP distribution for that of the IEEE 57 and 300 systems; while for NYISO system, Lognormal-clip and DPLN-clip fit best the data. This is also reasonable because, even if not one to one, the line impedance usually grows with the geographic distance between the buses it connects.

In addition, it is well known that the distribution of human settlements tend to be clustered; thus it is reasonable that long tails appear between these clusters of smaller size buses, giving rise to these heavy tails. This observation seems to agree with the topological properties found in the power grid graphs, and it is reasonable to consider these heavy weight impedances as good candidates for line impedances of the links that are rewired in the small world islands, as well as the ones connecting difference islands in our *nested- Smallworld* model, which is introduced in the next section.

Table 1.4. PDF Fitting for the Line Impedances in the IEEE and NYISO Power Grids

System	Fitting Distribution	ML Parameter Estimates ($alph$=0.05)
IEEE-30	$\Gamma(x\|a,b)$	$a = 2.14687$ $b = 0.10191$
IEEE-118	$\Gamma(x\|a,b)$	$a = 1.88734$ $b = 0.05856$
IEEE-57	$gp(x\|k,\sigma,\theta)$	$k = 0.33941$ $\sigma = 0.16963$ $\theta = 0.16963,$
IEEE-300	$gp(x\|k,\sigma,\theta)$	$k = 0.45019$ $\sigma = 0.07486$ $\theta = 0.00046,$
NYISO-2935	$logn_{clip}(x\|\mu,\sigma,Z_{\max})$	$\mu = -2.37419$ $\sigma = 2.08285$ $Z_{max} = 1.9977$
	$dPlN_{clip}(x\|\alpha,\beta,\mu,\sigma,Z_{\max})$	$\alpha = 44.25000$ $\beta = 44.30000$ $\mu = -2.37420$ $\sigma = 2.082600$ $Z_{max} = 1.9977$

1.5 A Model to Generate Random Topology Test Networks

There are a number of works in the power network literature that propose models to generate scalable-size power grid test cases, such as: the use of ring-structured grids to study the propagation pattern of disturbances [15]; a Tree-structured power grid model for detecting critical transitions in the transmission network which cause cascading failure blackouts [11]; the Watts-Strogatz *small-world* network [1]; or formation of a power grid topology starting from a Uniform and a Poisson distribution for the nodal location respectively (emulating what is often done in modeling wireless networks)[19]. While these proposed models provide some good perspectives to power grid characteristics, the generated topology fails to correctly or fully reflect that of a realistic power system

This section presents a random topology power grid model, RT-*nested-Smallworld*, which constructs a large scale power grid using a hierarchical way: first form connected sub-networks with size limited by the connectivity require-
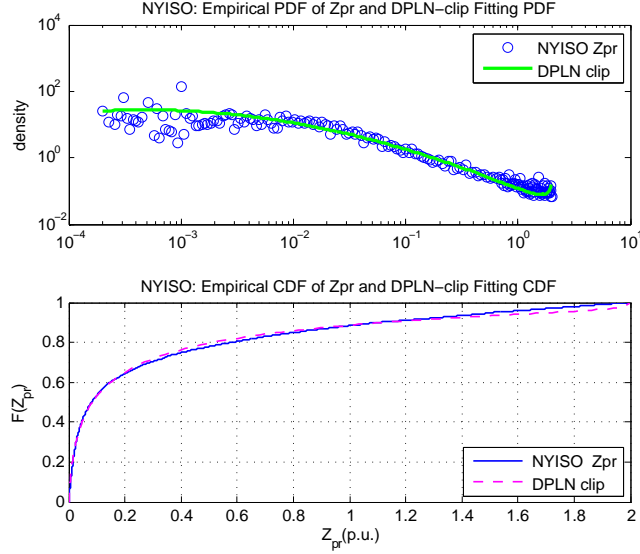
Figure 1.6 Comparison between Empirical PDF/CDF Distributions and Fitting Distributions: (a) IEEE 300; (b) NYISO 2935

ment; then connect the sub-networks through lattice connections; finally, generate the line impedances from some specific distribution and assign them to the links in the topology network. The hierarchy in the model is aroused from observation of real-world power grids: usually a large scale system consists of a number of smaller-size subsystem (e.g. control zones), which are interconnected by sparse and important tie lines. The model mainly contains three components: (a) *clusterSmallWorld* sub-network, (b) *Lattice*-connections, and (c) Generation and assignment of line impedances; which will be respectively described in details in following subsections.

1.5.1   clusterSmallWorld sub-Network

Electrical power grid topology has "*small-world*" characteristics; it is sparsely connected with a low average nodal degree which does not scale with the network size. On the other side, in order for a *small-world* model to generate a connected topology, the network size has to be limited. In this proposed model, different mechanisms from that of the Watts-Strogatz *Small-world* model have been adopted to form a power grid subnetwork in order to improve its resulting connectivity, as shown in the following paragraphs. Consequently, the connectivity limitation on the network size can be expanded from what is indicated by equation (1.9). The experiments have shown that: for $\langle k \rangle = 2 \sim 3$, the network size should be limited no greater than 30; and for $\langle k \rangle = 4 \sim 5$, 300.

Therefore the first step of this new model is to select the size of sub-networks according to the connectivity limitation. Then a topology is built up through a

modified *small-world* model, called *clusterSmallWorld*. This model is different from the Watts-Strogatz Small-world model in two aspects: the link selection and the link rewires. That is, instead of selecting links to connect most immediate $\langle k \rangle/2$ neighbors to form a regular lattice, it selects a number k of links at random from a local neighborhood N_{d_0} with the distance threshold of d_0, where k comes from a Geometric distribution. The local neighborhood is defined as the group of close-by nodes with mutual node number difference less than the threshold d_0, that is, $N_{d_0}^{(i)} = \{j;\ |j - i| < d_0\}$ for node i. It is worth noting that the clusterSmallWorld model adopts a Geometric distribution with the expectation of $\langle k \rangle$ for the initial node degree settings (i.e, for the link selection). The experiments have shown that the process of link selection and link rewiring that follows will transform the initial node degree distribution and finally result in a distribution with good matching approximation to the observed ones.
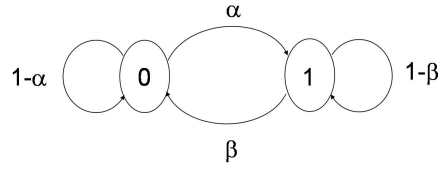

Figure 1.7 Markov Chain for Selecting Cluster of Rewiring Nodes (0: not rewire; 1: rewire)

For the link rewired, the Watts-Strogatz Small-world model selects a small portion of the links to rewire to an arbitrary node chosen at random in the entire network to make it a *small-world* topology. The clusterSmallWorld model uses a Markov chain with transition probabilities of (α, β), as shown in Fig. 1.7, to select clusters of nodes and therefore groups of links to be rewired. This mechanism is introduced in order to produce a correlation among the rewired links. After running above Markov transition for n times (i.e., one for each node in the network), we get clusters of nodes with "1"s alternating with clusters of nodes with "0"s, where "1" means to rewire and "0" means not. Then by a specific rewiring probability q_{rw}, some links are selected to rewire from all the links originating from each 1-cluster of nodes; and the corresponding local links get rewired to outside 1-clusters. The average cluster size for rewiring nodes is $K_{clst} = 1/\beta$; and the steady-state probabilities are $p_0 = \beta/(\alpha + \beta)$, $p_1 = \alpha/(\alpha + \beta)$. Experiments are performed on the available real-world power grid data to estimate the parameters. The average rewiring cluster size K_{clst}, the rewiring probability of links q_{rw}, and the ratio of nodes having rewire links p_1 can be directly obtained from statistical estimates. Then the transition probability can be computed as $\beta = 1/K_{clst}$ and $\alpha = \beta p_1/(1 - p_1)$.
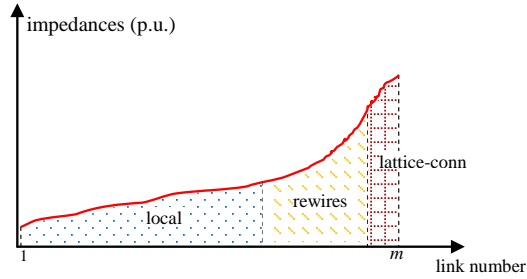
Figure 1.8 Grouping Line Impedances

1.5.2   Lattice-connections

The lattice-connections are selected at random from neighboring sub-networks to form a whole large scale power grid network. The number of lattice-connections between neighboring sub-networks is randomly chosen to be an integer with the mean of $\langle k \rangle$.

1.5.3   Assignment of Line Impedances

At this step m line impedances are generated from a specified heavy-tailed distribution, and then sorted by magnitude and grouped into local links, rewire links and lattice-connection links according to corresponding portions, as shown in Fig. 1.8. Finally line impedances in each group are assigned at random to the corresponding group of links in the topology.

1.6   Topological Analysis for the Distribution Networks

Usually the transmission network of a power grid is referred as High Voltage (HV) network with voltage levels above 50 kV. The studies and analysis in this chapter have been so far focused the HV transmission network of a power grid. Now we extend the topological analysis to the distribution side of the power grid. A distribution network carries electricity from the transmission system and delivers it to end users. Typically, the network would include MV (less than 50 kV) lines, electrical substations and pole-mounted transformers, LV (less than 1 kV) distribution wiring and sometimes electricity meters. The results are presented based on a sample 396-node Medium Voltage (MV) distribution network which comes from a real-world US distribution utility mainly located in a rural area.
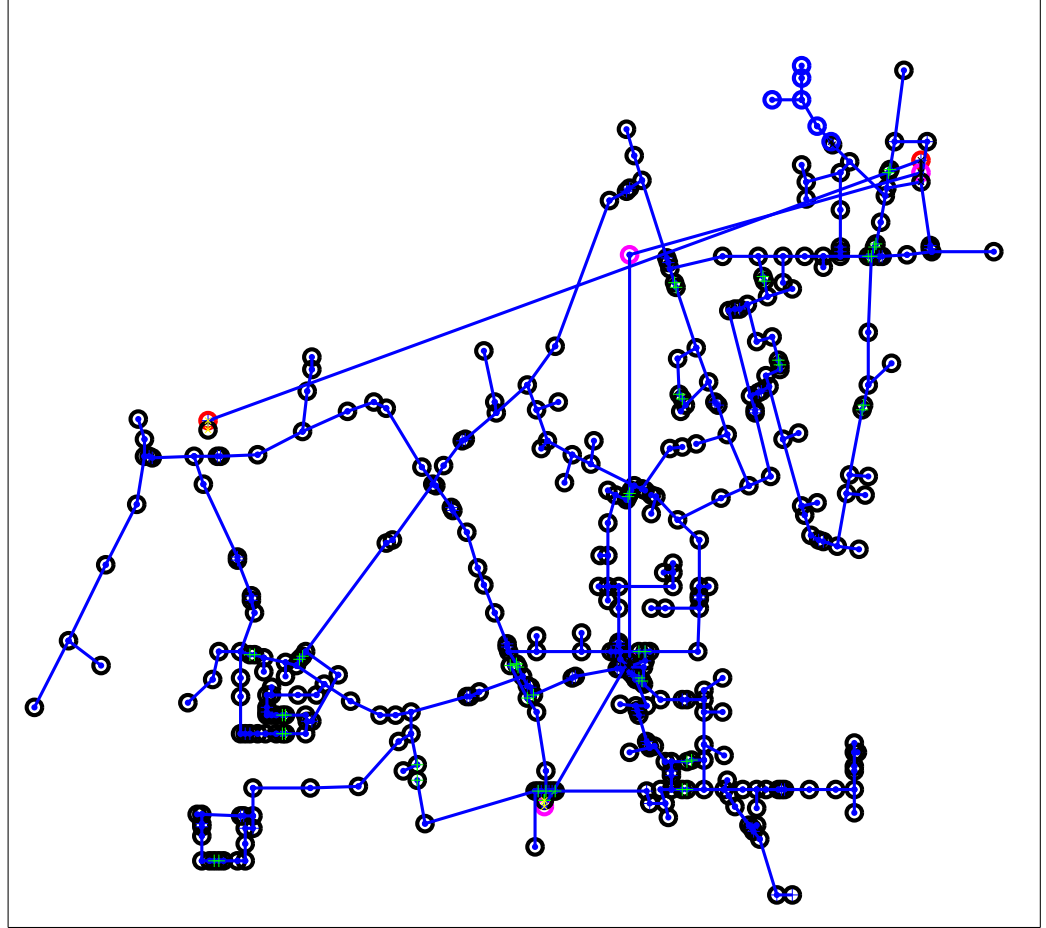
Figure 1.9 A 396-node MV distribution network in a rural area of the US. Components: bus (circle), line branches (line ending with dots), switches (line ending with '+'s), transformers (lines ending with 'x's), open or out of service component (green dotted line); the node color representing its voltage levels: 115 kV (red), 34.5 kV(magenta), 12.47 kV(black), 4.80 kV(blue).

1.6.1   Structure of the Distribution Network

In the low and medium voltage sections of the grid the physical layout is often restricted by what land is available and its geology. The logical topology can vary depending on the constraints of budget, requirements for system reliability, and the load and generation characteristics. Generally speaking, there are a few typical kinds of topology in the distribution network: ring, radial or interconnected.

A radial network is the cheapest and simplest topology for a distribution grid, and the one more often encountered. This network has a tree shape, in which power from a large supply radiates out into progressively lower voltage lines until the destination homes and businesses are reached. It is typical of long rural lines with isolated load areas. Today's grid is radially operated with respect to the current transmission system, but this topology will not hold anymore when Distributed Energy Resources (DER) will be integrated into the grid. Unfortunately this topology is the worst in terms of maximum communication delay because the number of hops between its nodes tend to grow in the order of the size of the network.

An interconnected or ring network is generally found in more urban areas and will have multiple connections to other points of supply. These points of connection are normally open but allow various configurations by the operating utility by closing and opening switches. Operation of these switches may be by remote control from a control center or by a lineman. The benefit of the interconnected model is that, in the event of a fault or a required maintenance, a small area of the network can be isolated and the remainder kept on supply.

Most areas provide three phase industrial service. A ground is normally provided, connected to conductive cases and other safety equipment, to keep current away from equipment and people. Distribution voltages vary depending on customer need, equipment and availability. Within these networks there may be a mix of overhead line construction utilizing traditional utility poles and wires and, increasingly, underground construction with cables and indoor or cabinet substations. However, an underground distribution network is significantly more expensive than lines deployed through an overhead construction. Distribution feeders emanating from a substation are generally controlled by a circuit breaker which will open when a fault is detected. Automatic circuit reclosers may be installed to further segregate the feeder thus minimizing the impact of faults. It is important to remark that long feeders experience voltage drop, and thus require the installation of capacitors or voltage regulators.

1.6.2   Graph Theoretic Analysis of a Sample MV Distribution Network

The logical topology of the sample 396-node MV distribution network analyzed here is shown in Figure 1.9. The power supply comes from the 115 kV-34.5 kV step-down substation. Most nodes or buses in the network are 12.47 kV, and only a small number of them are 34.5 kV or 4.8 kV. As shown in Figure 1.9, an MV network usually comprises different voltage levels, separated by transformers.

In the following topology analysis of the sample MV network, it is assumed that wireless or wired couplers have been implemented at the locations of transformers and switches, so that the network connectivity will not be affected by transformer types or switch status. On the other hand, if couplers are missing, the network will be segmented into several sections either by the transformers or by the open switches. For the sample MV network analyzed here, most buses ($> 95\%$) in

Table 1.5. Topological Characteristics of the Transmission Networks and the MV Distribution Network.

	n	$\langle k \rangle$	$\langle l \rangle$	ρ	$\lambda_2(L)$	$C(G)$	$C(R)$
IEEE-300	300	2.73	9.94	-0.2206	0.0094	0.0856	0.009119
WSCC	4941	2.67	18.70	0.0035	0.00076	0.0801	0.000540
MV-Distr	396	2.12	21.10	-0.2257	0.00030	0.0000	0.005367

the network are at the same voltage level of 12.47 kV. Therefore the topology analysis result of the separated 12.47 kV subnetwork is in fact very close to that of the whole connected graph.

The topology metrics we evaluated include the following:

- (n, m): the total number of nodes and branches, which well represents the network size.
- $\langle k \rangle$: the average node degree, which represents the average number of branches a node connects to.
- $\langle l \rangle$: the average shortest path length in hops between any pair of nodes.
- ρ: the Pearson correlation coefficient, which evaluates the correlation of node degrees in the network. This measure reflects if a node adjacent to a highly connected node has also a large node degree.
- $\lambda_2(L)$: the algebraic connectivity, which is the second smallest eigenvalue of the Laplacian matrix and is an index of how well a network is connected and how fast information data can be shared across the network.
- $C(G)$: the clustering coefficient, which assesses the ratio of nodes tending to cluster together.

The result of the analysis is listed in Table 1.5 with comparison to other two transmission networks: the IEEE-300 system represents a synthesized network from the New England power system and has a comparable network size as the 396-node MV distribution network we analyzed; the Western System Coordinating Council (WSCC) grid is the interconnected system of transmission lines spanning the Western United States plus parts of Canada and Mexico and contains 4941 nodes and 6594 transmission lines. It is well known that transmission and distribution topologies differ, nevertheless to comment on these differences in a quantitative manner as this exercise is useful for several reasons. For example, it allows us to better understand the characteristics of the transmission and distribution networks as information sources; it allows us to optimize the design of the distribution PMU based WAMS rather than attempting to duplicate the existing transmission one which is tailored to a network with very different topological characteristics; it can tells us how the distribution topology can be "modified" to achieve some advantageous characteristics of the transmission network, i.e. shorter path lengths between nodes, better algebraic connectivity, etc.

From Table 1.5 we can see that the 396-node MV distribution network has an average node degree of $\langle k \rangle = 2.12$, which is comparable to, although a little bit lower than, that of the other two transmission networks, the IEEE-300 system and the WSCC system. That means its average connecting sparsity is about at the same level as the compared transmission networks. However, the sample MV distribution network has a much longer average path length of $\langle l \rangle = 21.10$ in hops than the IEEE-300 system and, interestingly, it is even longer than that of the much larger 4941-node WSCC system. More specifically, any node in this MV distribution network is about 16.50 hops away from node-1 or node-2 which are 115-KV buses at the HV side of the two step-down supply transformers and may likely serve as the traffic sinks in the PLC-based network.

Looking at the algebraic connectivity $\lambda_2(L)$, the 396-node MV distribution network has a much weaker overall connectivity compared to the transmission networks, i.e. $\lambda_2(L) = 0.00030$ versus 0.0094 (IEEE-300) and 0.00076 (WSCC). This result shows that this topology is highly prone to become a disconnected graph under node failure (islanding). Finally, the most distinctive difference we found lies in the fact that the 396-node MV distribution network has a clustering coefficient equal to zero, compared to the clustering coefficient of 0.0856 for the IEEE-300 system and 0.0801 for the WSCC system. This means that no node in the sample MV distribution network is the vertex of a complete subgraph (triangle). MV distribution networks not located in rural areas are generally less prone to becoming a disconnected graph as in urban areas it is not unusual that utilities provide link redundancy, e.g. adding rings. If the distribution network becomes a disconnected graph, data connectivity obviously suffers if PLC is used. This vulnerability of the distribution network can be alleviated by adding judiciously wireless links to complement the PLC based network with the goal of improving network connectivity as well as shortest path lengths characteristics.

The average node degree of a power grid transmission network tends to be quite low and does not scale as the network size increases. The topology of a transmission network has salient *small-world* properties, since it features a much shorter average path length (in hops) and a much higher clustering coefficient than that of Erdös-Rényi random graphs with the same network size and sparsity. While small-world features have been recently confirmed for the HV transmission network , the sample MV network used here implies that a power grid distribution network has a very different kind of topology than that of a HV network and obviously it is not a *small-world* topology.

The node degree distribution of the 396-node MV distribution networkshows that: the maximum node degree in the network equals to 4 - which is much smaller than what is found in the transmission side of the grid where maximum nodal degrees of 20 or 30 can be found; about 16% of the nodes connect to only one branch, 60% connect with 2 branches, 22% with 3 branches, and only 2% with 4 branches.

Figure 1.4(e) depicts the network's spectral density, which is a normalized spectral distribution of the eigenvalues of its adjacency matrix. The spectrum of an
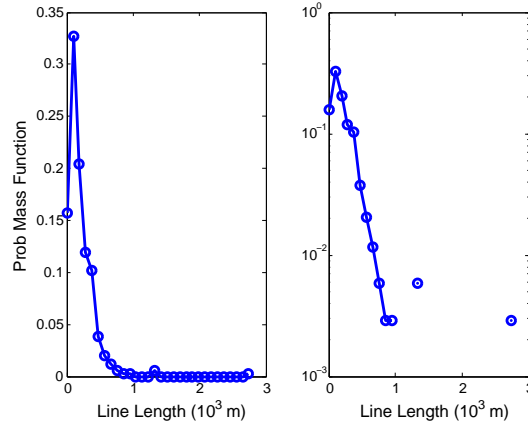
Figure 1.10 The probability mass function of the line length in the sample 396-node MV distribution network: (left) probability versus length; (right) log-probability versus length, where the existence of an exponential trend in the tail is clearly visible.

Erdös-Rényi random graph network, which has uncorrelated node degrees, converges to a semicircular distribution (see the semi-circle dotted line on the background in Figure 1.4(e)). The spectra of real-world networks have specific features depending on the details of the corresponding models.In particular, scale-free graphs develop a triangle-like spectral density with a power-law tail; whereas a small-world network has a complex spectral density consisting of several sharp peaks. The plot in Figure 1.4(e) indicates that the sample MV distribution network is neither a scale-free network nor a small-world network.

The branch lengths in the MV distribution network is also analyzed. The corresponding probability mass function is shown in Figure 1.10. It indicates that most of the branches are shorter than 1,067 m (3,500 ft) and the branch length distribution has an exponential tail with only a very small number of branches of extremely long length.

1.6.3   The LV Distribution Network

It is difficult to obtain example data about LV distribution network topologies. Generally speaking, an LV distribution network is radial, and has a similar network topology as an MV distribution network except that it may have more nodes with shorter branch length.

1.7   Summary

This chapter presents a comprehensive study on both the topological and electrical characteristics of electric power grids. It is found that the HV transmission network of power grid is sparsely connected with a low average node degree which

does not scale with the network size; the power grid topology manifests obvious *small-world* properties but its *small-world* rewires are not independent, as in that of the Watts-Strogatz *small-world* model; instead, the long hauls appear among clusters of nodes. This chapter provides evidence that the nodal degrees follow a mixture distribution which comes from the sum of a truncated Geometric random variable and an irregular Discrete random variable. It also proposes a method to estimate the distribution parameters by analyzing the poles and zeros of the average probability generation function. This chapter studies the graph spectral density and shows that power grid network takes on a distinctive pattern for its graph spectral density. The study on the algebraic connectivity of power networks has shown that power networks are exceptionally well connected given their sparsity, featuring a better scaling law than the Watts-Strogatz *small-world* graphs. It is shown that the distribution of line impedances is heavy-tailed and can be captured quite accurately by a clipped Double Pareto LogNormal (DPLN) distribution. This chapter introduces a novel random topology power grid model, RT-*nested-Smallworld*, intending to capture above observed characteristics.

At the end this chapter extends the same topological analysis to the distribution side of the power grid and reports the results based on a sample 396-node MV distribution network which comes from a real-world US distribution utility mainly located in a rural area.

References

[1] D. J. Watts, S. H. Strogatz, "Collective dynamics of 'Small-World' networks," *Nature*, volume 393, 1998, pp.393-440.

[2] R. Solé, M. Rosas-Casals, B. Corominas-Murtra, and S. Valverde, "Robustness of the European power grids under international attack," *Physics and Society (physics.soc-ph)*, http://arxiv.org/abs/0711.3710, 2007, (submitted).

[3] Z. Wang, A. Scaglione, R. J. Thomas, "The Node Degree Distribution in Power Grid and Its Topology Robustness under Random and Selective Node Removals", *1st IEEE International Workshop on Smart Grid Communications (ICC'10SGComm)*, Cape Town, South Africa, May 2010.

[4] R. Albert, I. Albert, and G. L. Nakarado, "Structural Vulnerability of the North American Power Grid," *Physical Review E*, volume 69, 2004, pp.1-4.

[5] P. Crucittia, V. Latorab, M. Marchioric, "A Topological Analysis of the Italian Electric Power Grid," *Physica A*, volume 338, 2004, pp.92-97.

[6] E. W. Dijkstra, "A note on two problems in connexion with graphs," *Numerische Mathematik*, volume 1, 1959, pp.269-271.

[7] J. L. Rodgers, and W. A. Nicewander, "Thirteen ways to look at the correlation coefficient," *The American Statistician*, volume 42(1), 1988, pp.59-66.

[8] M. Newman, "The structure and function of complex networks," *SIAM Review*, volume 45, 2003, pp.167-256.

[9] D. E. Whitney , D. Alderson, "Are technological and social networks really different," *Proc. 6th International Conference on Complex Systems (ICCS06)*, Boston, MA, 2006.

[10] R. Albert and A. Barabási, "Statistical mechanics of complex networks," *Reviews of Modern Physics*, volume 74(1), 2002, pp.47-97.

[11] B. A. Carreras, V. E. Lynch, I. Dobson, and D. E. Newman, "Critical points and transitions in an electric power transmission model for cascading failure blackouts," *Chaos*, volume 12(4), 2002, pp.985-994.

[12] P. Erdös, and A. Rényi, "On random graphs. I.," *Publicationes Mathematicae*, volume 6, 1959, pp.290-297.

[13] M. Fiedler, "Laplacian of graphs and algebraic connectivity," *Combinatorics and Graph Theory*, Banach Center Publications, Warsaw, volume 25, 1989, pp.57-70.

[14] E. J. Kirk, "Count loops in a graph," *http://www.mathworks.com/matlabcentral/fileexchange/10722*, 2007.

[15] M. Parashar, J. S. Thorp, "Continuum modeling of electromechanical dynamics in large-scale power systems," *IEEE Trans. on Circuits and Systems*, volume 51(9), 2004, pp.1848-1858.

[16] Power systems test case archive, (on line), http://www.ee.washington.edu/research/pstca/

[17] W. J. Reed, and M. Jorgensen, "The double pareto-lognormal distribution: a new parametric model for size distributions," *Communications in statistics, Theory and methods*, volume 33(8), 2004, pp.1733-1753.

[18] M. Rosas-Casals, S. Valverde, and R. Solé, "Topological vulnerability of the European power grid under erros and attacks," *International Journal of Bifurcations and Chaos*, volume 17(7), 2007, pp.2465-2475.

[19] Z. Wang, R. J. Thomas, A. Scaglione, "Generating random topology power grids," *Proc. 41st Annual Hawaii International Conference on System Sciences (HICSS-41)*, volume 41, Big Island, Jan 2008.

[20] E. P. Wigner,"Characteristic Vectors of Bordered Matrices with Infinite Dimensions," *The Annals of Math*, volume 62, 1955, pp.548-564.

[21] E. P. Wigner, "On the Distribution of the Roots of Certain Symmetric Matrices," *The Annals of Math*, volume 67, 1958, pp.325-328.